INCIPIENT SHORT CIRCUIT FAULT IMPACT ON SERVICE CONTINUITY OF AN ELECTRIC VEHICLE PROPELLED BY DUAL INDUCTION MOTORS STRUCTURE

S. YAHIA CHERIF[1] **D. BENOUDJIT**[1,2]
[1]LSP-IE'2000 Laboratory, Electrical Engineering department, University of Batna 2
Rue Chahid M[ed] El-Hadi Boukhlouf 05000 Batna, Algeria, Tél./Fax: +213 33 81 51 23

M.S. NAIT-SAID[1] **N. NAIT-SAID**[1]
[2]Health and Safety Institute, University of Batna 2, 53 route de Constantine, Batna, Algeria, Tél./Fax: +213 33 23 01 43

Abstract: *The short circuit is among one of the most dangerous electrical faults in induction motor, which leads to serious implications on the motor operation and its performances. The present paper deals with the influence of the stator short circuit fault in its early stage in terms of performances and service continuity of an electric vehicle (EV) using dual induction motor's structure piloted by Backstepping control. An equivalent induction motor model with turn-to-turn fault on one stator phase, without already assuming the temperature effect through an intrinsic model, is investigated and thereafter its impacts on electric vehicle performance using simulation tests are presented and discussed.*

Key words: *Backstepping control, Electric vehicle (EV), turn-to-turn-fault, Propulsion control structure.*

1. Introduction

A motor control system with high robustness is an important issue in research [1]. Thus, it is obvious that the monitoring and diagnosis of electrical machine constitute an economic and scientific challenge, combining safety and continuity of service for electrical drives. About 35% to 40% of the total failures of induction motor take place due to electrical faults [2]. The stator winding insulation failure due to a short-circuit known as inter turn short-circuit is one of the most common and severe kind of electrical faults affecting the electric motor [3-5]. This is mainly due to long term thermal aging and ultimately insulation failure [2]. If the turns of stator are shorted a large circulating current induced in shorted turn so the thermal overloading [6]. However, during operational phases, electric motors are continuously being exposed to thermal, mechanical and vibrational effects.

Therefore, it is important to detect and identify any incipient fault that occurs within the electrical motor at its earliest stage to avoid any unplanned outage, particularly in applications where safety is the primary concerns the global system. On the over side, it is common for any vehicle in urban traffic requires regime changes, frequent acceleration, deceleration, cruising, and stopping phases, which lead to serious breakdowns. In those applications where downtime isn't acceptable and where continuity of service is required, an unpredicted failure of a motor might result in higher maintenance costs or loss of life. However, understanding fault diagnosis is very important, because a good diagnosis is an early detection of the severity and location of faults, to reduce the downtime as well as the maintenance costs while ensuring continuity of operations for an EV. Therefore, modeling and identification of inter-turn short circuit fault at its earliest stage of an induction motor is the first major step in the motor health monitoring and fault diagnosis process. The main focus of the present work is on the influence of an incipient inter turn short circuit fault occurred at its earliest stage on electric vehicle performances and service continuity. The proposed control structure consists of an electric vehicle using dual-induction motors Backstepping control placed at the rear wheels, which propels electrically the vehicle, based on an electric differential assured by dual motors operating at different speed. For this purpose, a precise equivalent model of an induction motor (IM) taking into account the presence of the turn-to-turn fault resulting of a short-circuit winding in stator phase at several levels is described, and the consequences on electric vehicle performances in terms of service continuity where a fault occurred into one of both propulsion structure motors are analyzed.

Simulation tests were carried out for detecting fault occurrence and its impact on EV control, without already considering the temperature effect through an intrinsic model, for a faulty model. Also, note that the existence of the short-circuit in some turns on one phase could give an increase in temperature inside the machine leading to overheating which causes the insulation loss of the machine winding and the short circuit becomes rapid and total in such a small time.

The paper is organized as follows. Section 2 presents the Backstepping control for IM, using an accurate faulty model with turn-to-turn fault applied for an EV. In section 3, the dual-motor configuration of the proposed propulsion structure will be shown. To evaluate the performances and the failures effect caused by turn-to-turn fault in first stator phase of the right motor, series of simulation tests will be presented in section 4. Conclusion is done in section 5.

2. Backstepping control for IM

Backstepping control technique enables in a sequential and systematic manner to build stabilizing Lyapunov function. Thus, the main goal is to achieve the convergence of errors towards zero and stable operations of the system. The design of Backstepping control approach is to recursively select the appropriate state variables as virtual reference input, characterized by step-by-step interlacing. Each step generates a new virtual control variable and finally the process terminates when the final external control is reached [7-11].

Let us first given the equations of an IM for a healthy model, which includes both the mechanical and electrical dynamics, expressed in the (d,q) synchronous rotating frame obviously, after orientation of the rotor flux by [1][8]:

$$\begin{cases} \dfrac{d\Omega}{dt} = \dfrac{pM}{JL_r}\phi_r i_{sq} - \dfrac{T_L}{J} \\ \dfrac{d\phi_r}{dt} = \dfrac{M}{T_r} i_{sd} - \dfrac{1}{T_r}\phi_r \\ \dfrac{di_{sd}}{dt} = -\left(\dfrac{R_s}{\sigma L_s} + \dfrac{M^2 R_r}{\sigma L_s L_r^2}\right) i_{sd} + \omega_s i_{sq} + \dfrac{MR_r}{\sigma L_s L_r}\phi_r + \dfrac{1}{\sigma L_s} v_{sd} \\ \dfrac{di_{sq}}{dt} = -\left(\dfrac{R_s}{\sigma L_s} + \dfrac{M^2 R_r}{\sigma L_s L_r^2}\right) i_{sq} - \omega_s i_{sd} - \dfrac{MR_r}{\sigma L_s L_r}\phi_r + \dfrac{1}{\sigma L_s} v_{sq} \end{cases} \quad (1)$$

The objective of the Backstepping design is to synthesize the d-axis and q-axis voltage control input expressions (v_{sd}^*, v_{sq}^*), where the system must be able to follow the desired references. It mainly consists of the following two steps.

For the first step, the objective is the replacement of classical PI tracking controller by computing the reference values of stator current components (i_{sd}^*, i_{sq}^*). In our case, the tracking errors dynamics of speed $\dot{e}_\Omega$ and rotor flux $\dot{e}_\phi$, by using equations (1) are defined as follows:

$$\begin{cases} \dot{e}_\Omega = \dot{\Omega}^* - \dot{\Omega} = \dot{\Omega}^* - \dfrac{1}{J}\dfrac{pM}{L_r}\phi_r i_{sq} + \dfrac{T_L}{J} \\ \dot{e}_\phi = \dot{\phi}_r^* - \dot{\phi}_r = \dot{\phi}_r^* - \dfrac{M}{T_r} i_{sd} + \dfrac{1}{T_r}\phi_r \end{cases} \quad (2)$$

Then, with an appropriate choice of the Lyapunov function V_1 of the subsystem described above, such that:

$$V_1 = \frac{1}{2}\left(e_\Omega^2 + e_\phi^2\right) \quad (3)$$

For which its derivative $\dot{V}_1$ must be negative, we can write:

$$\begin{cases} \dot{e}_\Omega = -k_\Omega \cdot e_\Omega \\ \dot{e}_\phi = -k_\phi \cdot e_\phi \end{cases} \quad (4)$$

where k_Ω, k_ϕ are positives coefficients in order to guarantee the stable tracking. Thereby, the reference values of stator current components are given by:

$$\begin{cases} i_{sd}^* = \dfrac{JL_r}{pM\phi_r}\left(\dot{\Omega}^* + k_\Omega \cdot e_\Omega + \dfrac{1}{J} T_r\right) \\ i_{sq}^* = \dfrac{T_r}{M}\left(\dot{\phi}_r^* + k_\phi \cdot e_\phi + \dfrac{1}{T_r}\phi_r\right) \end{cases} \quad (5)$$

In the second step, the main goal is to achieve the final external control, by computing the reference stator voltage. To do so, we define the stator current errors terms. Expressed by their derivatives as follows:

$$\begin{cases} \dot{e}_{id} = \dot{i}_{sd}^* - \dot{i}_{sd} \\ \dot{e}_{iq} = \dot{i}_{sq}^* - \dot{i}_{sq} \end{cases} \quad (6)$$

Substituting (1) into (6), we find:

$$\begin{cases} \dot{e}_{id} = \dot{i}_{sd}^* - d_1 - \dfrac{1}{\sigma L_s} v_{sd} \\ \dot{e}_{iq} = \dot{i}_{sq}^* - d_2 - \dfrac{1}{\sigma L_s} v_{sq} \end{cases} \quad (7)$$

Where

$$\begin{cases} d_1 = -\left(\dfrac{R_s}{\sigma L_s} + \dfrac{M^2 R_r}{\sigma L_s L_r^2}\right) i_{sd} + \omega_s i_{sq} + \dfrac{MR_r}{\sigma L_s L_r}\phi_r \\ d_2 = -\left(\dfrac{R_s}{\sigma L_s} + \dfrac{M^2 R_r}{\sigma L_s L_r^2}\right) i_{sq} - \omega_s i_{sd} - \dfrac{MR_r}{\sigma L_s L_r}\phi_r \end{cases} \quad (8)$$

From the equations system (7), the stator voltage input, could be calculated through the definition of another Lyapunov function into the following form:

$$V_2 = V_1 + \frac{1}{2}\left(e_{id}^2 + e_{iq}^2\right) \tag{9}$$

To ensure that its derivative is always negative, such that

$$\dot{V}_2 = \dot{V}_1 - k_{id}e_{id}^2 - k_{iq}e_{iq}^2 \tag{10}$$

with k_{id}, k_{iq} are positives coefficients.

Finally, the input voltages components are chosen as follows:

$$\begin{cases} v_{sd}^* = \sigma L_s (i_{sd}^* - d_1 + k_{id}e_{id}) \\ v_{sq}^* = \sigma L_s (i_{sq}^* - d_2 + k_{iq}e_{iq}) \end{cases} \tag{11}$$

For a faulty model, different research works of mathematical models regarding inter-turn short-circuit faults in the stator of an induction motors can be found in literature [12-14]. As the need for greater accuracy in induction motor modeling, important physical characteristics have to be taken into account. An accurate model for an induction motor with stator winding turn fault in first phase was presented in [14].

Stator, rotor and short circuit equations in matrix form for an IM faulty model in coordinates referred to the stator frame, with a turn-to-turn fault in the first phase "a", is formulated as follows [14], given next by equation (12). Index sc denotes short circuit. Conventional used abbreviation of the induction motor will be defined next in nomenclature.

$$v = D_{1sc}I + \left[\omega D_{2sc} + D_{3sc}\frac{dI}{dt}\right] \tag{12}$$

with:

$$D_{1sc} = \begin{bmatrix} R_s & 0 & 0 & 0 & -\sqrt{\frac{2}{3}}x_{sc}R_s \\ 0 & R_s & 0 & 0 & 0 \\ 0 & 0 & R_r & 0 & 0 \\ 0 & 0 & 0 & R_r & 0 \\ \sqrt{\frac{2}{3}}x_{sc}R_s & 0 & 0 & 0 & -(R_s + x_{sc}R_s) \end{bmatrix}$$

$$D_{2sc} = \begin{bmatrix} 0 & 0 & 0 & 0 & 0 \\ 0 & 0 & 0 & 0 & 0 \\ 0 & M & 0 & L_r & 0 \\ -M & 0 & -L_r & 0 & \sqrt{\frac{2}{3}}mx_{sc} \\ 0 & 0 & 0 & 0 & 0 \end{bmatrix}$$

$$D_{3sc} = \begin{bmatrix} L_s & 0 & M & 0 & 0 \\ 0 & 0 & 0 & M & 0 \\ M & 0 & L_r & 0 & -\sqrt{\frac{3}{2}}mx_{sc} \\ 0 & M & 0 & L_r & 0 \\ x_{sc}\sqrt{\frac{2}{3}}L_s & 0 & mx_{sc}\sqrt{\frac{3}{2}} & 0 & -x_{sc}^2 L_s \end{bmatrix}$$

The voltage and current matrices are expressed as:

$$v = \left[v_{s\alpha}\ v_{s\beta}\ 0_{r\alpha}\ 0_{r\beta}\ 0_{sc}\right]^T,\ I = \left[i_{s\alpha}\ i_{s\beta}\ i_{r\alpha}\ i_{r\beta}\ i_{sc}\right]^T.$$

The short-circuited turn's index is:

$$x_{sc} = \frac{n_{sc}}{n} = \frac{\text{Number of interturns short - circuit windings}}{\text{Total number of interturns in healthy phase}}$$

Figure 1 shows a general block diagram implementation of Backstepping control intended to EV application. This is used to maintain stability and better performance capabilities of the system under disturbances, with at least two control loops. As shown in Fig. 1, n_{sc} represents a number of shortened turns in the first stator phase "a". R_{sc} is an equivalent resistance of the shortened turns.

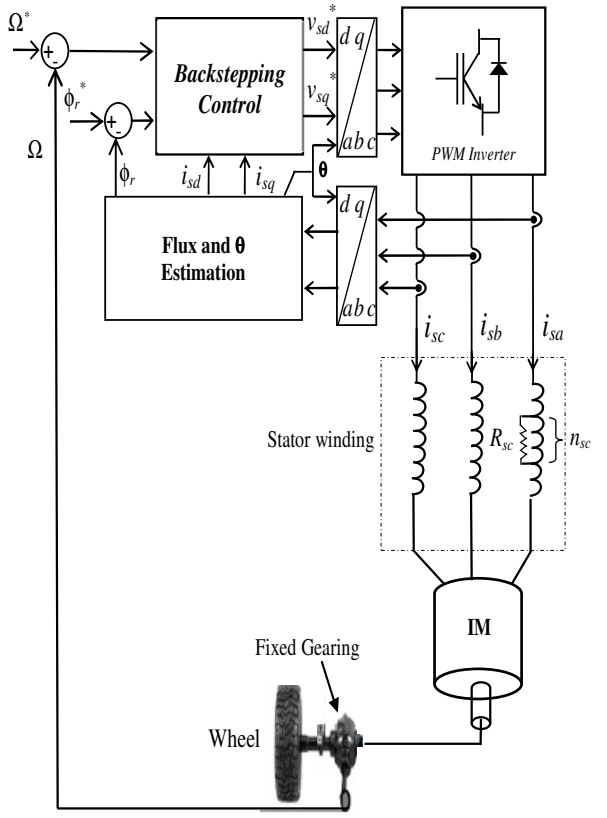

Fig. 1. Backstepping structure of IM with turn-to-turn fault on phase a.

When the short circuit fault is negligible ($x_{sc} = R_{sc} = 0$) the previous formulation gives exactly the same as in the healthy model.

3. Electric vehicle dual induction motor's structure

Figure 2 presents the proposed control structure in which two identical induction motors drive, separately the rear wheels of the vehicle via fixed gearing. The left and right induction motors are fed through power converters and driven by Backstepping strategy.

The differential action assured by dual motors operating at different speed enables the wheels to be driven at different speeds when cornering the outer wheel covering a greater distance than the inner wheel. Then the propulsion control structure placed at the rear wheels propels electrically the vehicle and assures the required differential speed Ω_{diff} according to [15]:

$$\begin{cases} \Omega_1^* = \Omega_o^* + \Omega_{diff}^* \\ \Omega_2^* = \Omega_o^* - \Omega_{diff}^* \end{cases} \quad (13)$$

where:

Ω_1^*, Ω_2^*: Speeds of left motor 1 and right motor 2.

Ω_o^*, Ω_{diff}^* : EV speed command, speed difference.

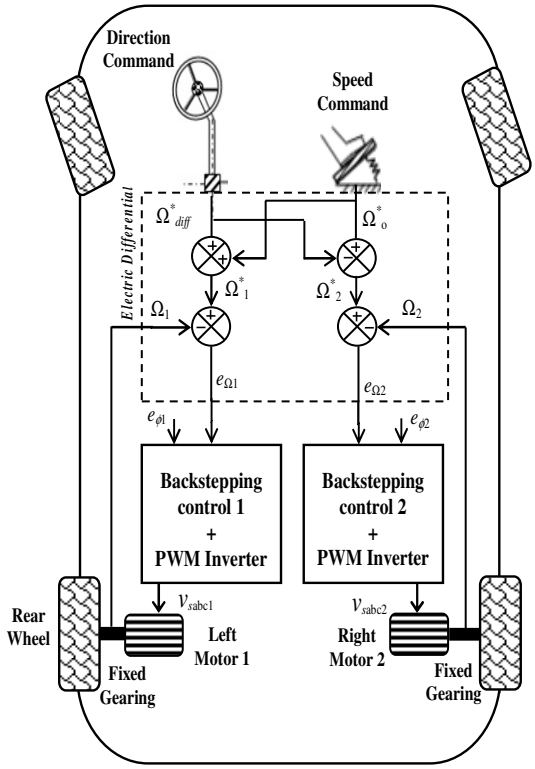

Fig. 2. EV propulsion control structure.

4. Simulation results and discussion

Numerical simulations have been carried out, in order to assess the effect of initial turn-to-turn fault on electric vehicle structure performances propelled by dual induction motors which rated data are summarized in the appendix.

Figures 3(a,b,c) and their respective zoom on Figures 3(a_1, b_1) also, Figures 3(a_2, b_2, c_2) depict and compare the main characteristics (speed, electromagnetic torque, stator currents and copper losses responses) of an EV propulsion structure using dual inductions motors driven by Backstepping control where the turn-to-turn fault resulting of a short-circuit winding may be occurred in the first stator phase into one of both propulsion motors structure (the right motor) at several short-circuited turns index levels: x_{sc} = 20%, 50% and 100%.

The simulation tests were used considering the selected route defined as illustrated in figures 3 by the vehicle speed reference drawn in dashed line.

From scratch, the vehicle starts with a constant acceleration until attains the speed of 157 rad/s then it will be maintained constant. In fact, in this propulsion structure each of both motors is associated with a fixed mechanical gearing, which enables the reduction of the motor speed to the desired wheel speed and high substantial torque.

At t = 0.5s, a load torque is applied on each motor. This last case might be occurred for example when EV wheels are stopped by a strong obstacle. After there, at t = 1s the vehicle accomplishes its turn maneuvers, by turning left.

The electric differential action allows the inner wheel to rotate slower than the outer one, i.e $\Omega_{Right} > \Omega_{left}$. Further, to test severely the propulsion structure performances, at t = 1.5s the turn-to-turn fault resulting of a short-circuit winding in the first stator phase has been activated on the right motor when the vehicle accomplishes its turn maneuvers.

Finally, the vehicle maintains a constant cruising speed, which results in equality of both motors speeds, i.e $\Omega_{Right} = \Omega_{left}$.

Figure 3a and its zoom in figure 3a1 show before and after the shorted turns faulty case for x_{sc} =20%, introduced at t = 1.5sec, the simulated EV speed, electromagnetic torque and stator currents waveforms.

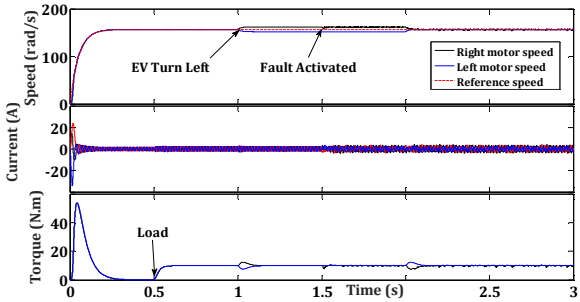

Fig. 3a. Turn-to-turn fault effect for x_{sc} = 20 %.

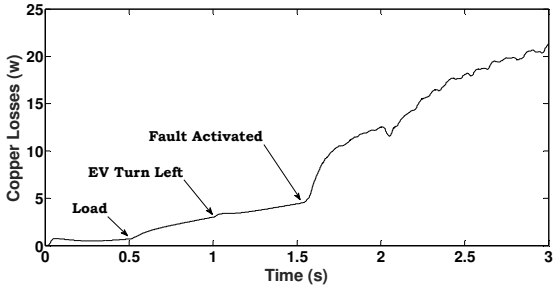

Fig. 3a$_2$. Cooper losses evolution for x_{sc} = 20 %.

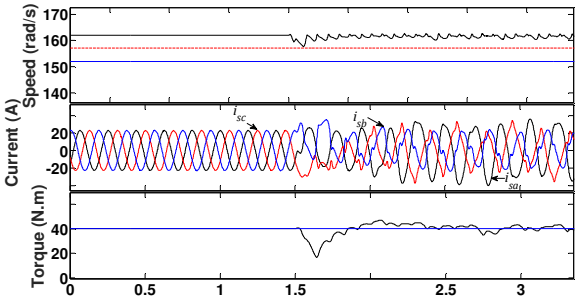

Fig. 3a$_1$. Zoom of turn-to-turn fault effect for x_{sc} = 20 %.

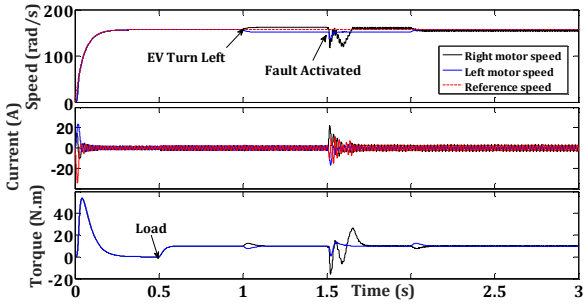

Fig. 3b. Turn-to-turn fault effect for x_{sc} = 50 %.

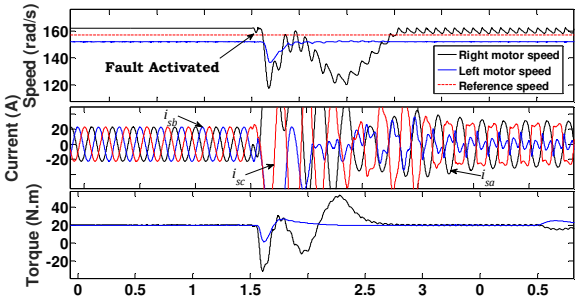

Fig. 3b$_1$. Zoom of turn-to-turn fault effect for x_{sc} = 50 %.

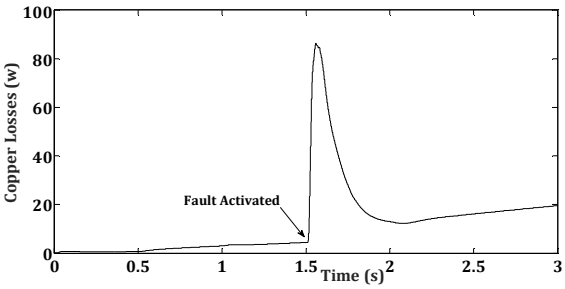

Fig. 3b$_2$. Cooper losses evolution for x_{sc} = 50 %.

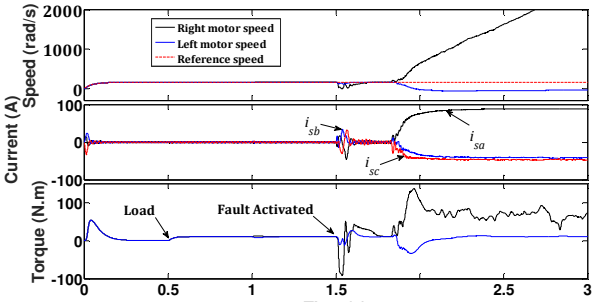

Fig. 3c. Turn-to-turn fault effect for x_{sc} = 100 %.

It can be seen that the fault effect in this case, isn't noticeable on the EV speed and electromagnetic torque responses, expect for the stator currents amplitudes, which increase slightly after fault occurs. So, in this case, the incipient winding fault will not impose great influences on EV performances.

Figure 3a$_2$ shows with the same above shorted turns faulty case for x_{sc} = 20%, the evolution of stator copper losses versus time. It is well known that copper losses dependent on the square of stator current in RMS value and the stator resistance. These losses result from Joule heating are caused by stator current induced in the stator windings, which generates the heat, and therefore the temperature of the motor rises with time. Indeed, as can be seen from Figure 3a$_2$ as the stator currents amplitudes increase, the copper losses increase also with time particularly when the fault occurs.

On the other hand, as shown in figures 3(b-c) and 3(b$_1$) the fault effect is more noticeable as the fault severity increases. For x_{sc} = 50%, and in particular, for x_{sc} = 100%, while the stator current amplitude of the faulty phase current becomes higher.

The increase in RMS stator currents may have a serious damage, such as total short-circuit of the stator winding, the degradation of the insulation of the windings due to the resulting overheating, which potentially shortening its lifespan and even fire.

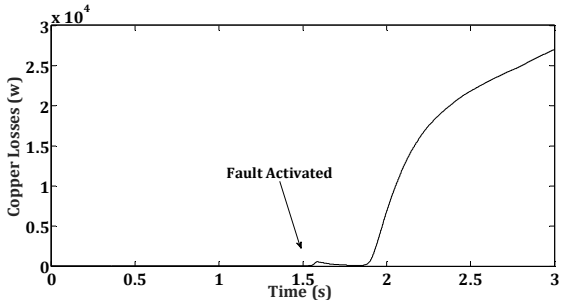

Fig. 3c$_2$. Cooper losses evolution for x_{sc} = 100 %.

At the same time, the occurred fault cited above might influence one of the dual induction motors which could be conducted an unbalance in the dual used motors and from which the vehicle leaves its reference trajectory, so the control of the differential action is gravely lost accompanied by the loss of the aim control vehicle direction. Finally, as depicted in figures 3(b$_2$, c$_2$) with rising amplitude currents the copper losses increase also.

5. Conclusion

In this paper, we focused on the incipient turn-to-turn fault influence on EV dual induction motor's structure performances and service continuity. An accurate model for an induction motor with inter-turn fault in the first phase of stator winding occurred into one of both motors has been presented for detecting fault occurrence and its impact on EV control, without already considering the temperature effect through an intrinsic model, for a faulty model. Simulation tests performed under a fault severity index at several levels show that the incipient turn-to-turn short fault has a small effect for a lower-level fault on EV operation. In this case, the vehicle continued to function even in the presence of fault. But for the high fault levels, the results show a very significant change, particularly for the currents wave forms. The stator currents amplitude raised significantly where the fault has occurred and a relative height that is lower for the other phases.

Thus, if no coping measures are applied, this will result in the temperature increase in the stator winding, which will lead to the failure of the entire phase eventually. That's means unfortunately the loss of the systematic control on the EV driven by the propulsion structure.

Nomenclature

v_s , i_s	Stator voltage, stator current αβ-vector
ϕ_s	Stator flux αβ-vector
R_s , R_r	Stator and rotor resistances
L_s , L_r	Global Stator and rotor self-inductances of each armature
M	Global Mutual inductance between stator and rotor armatures
m	Mutual inductance between two phases stator and rotor, where, $m = \frac{2}{3}M$
T_r	Rotor time constant where, $T_r = \frac{L_r}{R_r}$
ω_s	Synchronous angular speed
j	Imaginary unit, satisfying $j^2 = -1$
θ	Flux stator angle
p	Number of pole pairs
T_e , T_L	Electromagnetic torque, Torque Load
(.)*	Input command variable
i_s	Current flowing through the short circuit winding
Ω	Mechanical speed
Ω_1, Ω_2	Speeds of left motor and right motor
Ω^*_o, Ω_{diff}	EV speed command, speed difference
J	Rotor Inertia
PI	Proportional Integral controller

Appendix

Table 1 Induction motor parameters

Parameters	Values
Power	4 [kW]
Voltage	220/380 V
Frequency	50 Hz
+ Eventual three-phase boost transformer with ratio 1/20 adapted to voltage battery	
R_s	1.2 [Ω]
R_r	1.8 [Ω]
L_s=L_r	0.1564 [H]
M	0.15 [H]
J	0.07 [Kg.m2]
p	2

References

1. Roubache, T., Chaouch, S., Naït-Saïd, M.S.: *Backstepping design for fault detection and FTC of an induction motor drives-based EVs*. In: Automatika, (2016), Vol. 57, N° 3, p. 736–748.
2. Gangsar, P., Tiwari, R.: *Signal based condition monitoring techniques for fault detection and diagnosis of induction motors: A state-of-the-art review*. In: mechanical systems and signal processing, (October 2020), Vol. 144, p. 1–37.
3. Mazzoletti, M.A., Bossio, G.R., De Angelo, C.H., Espinoza-Trejo, D.R.: *A Model-Based Strategy for Inter turn Short-Circuit Fault Diagnosis in PMSM*. In: IEEE Transactions on Industrial Electronics, (September 2017), Vol. 64, N° 9, p. 7218–7228.
4. Wu, Y., Jiang, B., Wang, Y.: *Incipient winding fault detection and diagnosis for squirrel-cage induction*

motors equipped on CRH trains. In: ISA Transactions, (2020), Vol. 99, p. 488–495.
5. Teguia, J.B., God promesse Kenne, G.C.F.: *Induction Motor Windings Faults Detection Using Active and Reactive Power Based Model Reference Adaptive System Estimator*. In: International Journal of Progressive Sciences and Technologies (IJPSAT), (2 November 2020), Vol. 23, N°2, p. 66–86.
6. *Dhamal, S.S., Bhatkar, M.V.: Modelling and Simulation of Three-Phase Induction Motor to Diagnose the Performance on Inter-Turn Short Circuit Fault in Stator Winding*. In: International Conference on Computing, Power and Communication Technologies (GUCON), Sep 28-29, 2018, Greater Noida, UP, India, p. 1166–1172.
7. El Kharki, A., Boulghasoul, Z., Et-Taaj, L., Kandoussi, Z., Elbacha, A.: *Real Time Implemntation of Backstepping Control for High Performances Induction Motor Drive*. In: 4th World Conference on Complex Systems (WCCS), 22-25 April, 2019, Ouarzazate, Morocco.
8. Trabelsia, R., Khedher, A., Mimouni, M.F., M'sahli, F.: *Backstepping control for an induction motor using an adaptive sliding rotor-flux observer*. In: Electric Power Systems Research, December 2012, Vol. 93, p. 1–15.
9. Vaidyanathan, S., Azar, A.T.: *Backstepping Control of Nonlinear Dynamical Systems*, 1st edition, Academic Press, 15th august 2020, p. 1–515.
10. Horch, M., Boumediene, A., Baghli, L.: *Backstepping approach for nonlinear super twisting sliding mode control of an induction motor*. In: 3rd International Conference on Control, Engineering & Information Technology, IEEE CEIT'2015, 26 may 2015, Tlemcen, Algeria.
11. Ameid, T., Menacer, A., Romary, R., Pusca, R., Talhaoui, H.: *DWT for rotor bars fault detection applied to Backstepping control induction motor drive in low-speed*. In: 43th Annual Conference of the IEEE Industrial Electronics Society, Oct.-1 29 Nov. 2017, p. 8059–8064.
12. Dhamal, S.S., Bhatkar, M.V.: *Modelling and Simulation of Three-Phase Induction Motor to Diagnose the Performance on Inter-Turn Short Circuit Fault in Stator Winding*. In: International Conference on Computing, Power and Communication Technologies (GUCON), 28-29 Sept. 2018, p. 1166–1172, Greater Noida, India.
13. Hamoudi, A., Kouadri, B.: *On-Line Stator Winding Inter-Turn Short-Circuits Detection in Induction Motors Using Recursive Levenberg-Marquardt Algorithm*. In: International Journal on Electrical Engineering and Informatics, March 2017, Vol. 9, N°1, p. 42–57.
14. Bouakoura, M., Naït-Saïd, M.S., Naït-Saïd, N.: *Incipient Inter-Turn Short Circuit Fault Estimation Based on a Faulty Model Observer and ANN-Method for Induction Motor Drives*. In: Recent Advances in Electrical & Electronic Engineering, 2019, Vol. 12, p. 1–7.
15. Benoudjit, D., Nait-Said, N., Nait-Said, M-S.: *Differential Speed Control of a Propulsion System using Fractional-Order Controller*. In: Electromotion Journal, April-June 2007, Vol. 14, N° 2, p. 91–98.